

Attenuation of Intestinal Epithelial Cell Migration During *Cryptosporidium parvum* Infection Involves Parasite Cdg7_FLc_1030 RNA-Mediated Induction and Release of Dickkopf-1

Zhenping Ming,^{1,2} Yang Wang,² Ai-Yu Gong,² Xin-Tian Zhang,² Min Li,² Ting Chen,^{2,4} Nicholas W. Mathy,² Juliane K. Strauss-Soukup,³ and Xian-Ming Chen²

¹Department of Medical Parasitology, School of Basic Medical Sciences, Wuhan University, Hubei, China; ²Department of Medical Microbiology and Immunology, Creighton University School of Medicine, Omaha, Nebraska; ³Department of Chemistry, Creighton University College of Arts and Sciences, Omaha, Nebraska; and ⁴Department of Gastroenterology, Hubei University of Science and Technology, Hubei, China

Intestinal infection by *Cryptosporidium* is known to cause epithelial cell migration disorder but the underlying mechanisms are unclear. Previous studies demonstrated that a panel of parasite RNA transcripts of low protein-coding potential are delivered into infected epithelial cells. Using multiple models of intestinal cryptosporidiosis, we report here that *C. parvum* infection induces expression and release of the dickkopf protein 1 (Dkk1) from intestinal epithelial cells. Delivery of parasite Cdg7_FLc_1030 RNA to intestinal epithelial cells triggers transactivation of host *Dkk1* gene during *C. parvum* infection. Release of Dkk1 is involved in *C. parvum*-induced inhibition of cell migration of epithelial cells, including noninfected bystander cells. Moreover, Dkk1-mediated suppression of host cell migration during *C. parvum* infection involves inhibition of Cdc42/Par6 signaling. Our data support the hypothesis that attenuation of intestinal epithelial cell migration during *Cryptosporidium* infection involves parasite Cdg7_FLc_1030 RNA-mediated induction and release of Dkk1 from infected cells.

Keywords. *Cryptosporidium*; cryptosporidiosis; intestinal epithelium; parasitic infection; Dkk1; gene transcription; cell migration.

Cryptosporidium, a genus of protozoa in the phylum Apicomplexa, represents a group of protozoan parasites that can infect humans and many other species of animals [1, 2]. The *C. parvum* and *C. hominis* species cause most *Cryptosporidium* infections in humans, particularly in AIDS patients and in children younger than 2 years old in developing countries [1, 3]. Humans are infected when they ingest *Cryptosporidium* oocysts. Once ingested, oocysts excyst in the gastrointestinal tract and release infective sporozoites. The sporozoite attaches to a host epithelial cell and forms a vacuole in which the organism remains intracellular but extracytoplasmic. The internalized sporozoite then matures, undergoes asexual and sexual development, and yields oocysts to complete a life cycle within 4–6 days [2]. *Cryptosporidium* can complete all stages of its development (asexual and sexual) within a single host [2].

The primary infection site of the parasite in humans is the small intestine. The intestinal mucosa is a monolayer of rapidly self-renewing epithelial cells. New functional epithelial cells are

produced from stem cells in the crypt base, differentiate, and migrate from the crypt base to the luminal surface, and, eventually, are shed into the lumen after they have reached the tip of the villus; hence, the entire intestinal epithelium is replaced every 2–3 days in mice (3–5 days in humans) [4, 5]. It appears that *Cryptosporidium* has developed strategies to counteract the rapid turnover of intestinal epithelium to support its intracellular cell cycle. *C. parvum* infection induces apoptotic resistance in infected epithelial cells during the early stage of infection [6]. We recently observed that *C. parvum* infection inhibits cell migration of intestinal epithelial cells in culture, including infected cells and noninfected bystander cells [7]. Both the apoptotic resistance in infected cells and attenuation of epithelial cell migration may provide a survival benefit to the parasite cell cycle. However, molecular mechanisms underlying host cell migration inhibition during *Cryptosporidium* infection are still unclear.

The interactions between *Cryptosporidium* and intestinal epithelial cells involves exchanges of distinct effector molecules from both sides of the host cell and the parasite at the host-parasite interface [8, 9]. Such exchanges of effector molecules may be involved in parasite invasion and intracellular development [1, 8, 9]. In our previous studies [10], we demonstrated that several *C. parvum* RNA transcripts of low protein-coding potential are selectively delivered into intestinal epithelial cells during host-parasite interactions and may modulate gene transcription in infected host cells. Specifically, delivery

Received 28 February 2018; editorial decision 11 May 2018; accepted 31 May 2018; published online July 23, 2018

Correspondence: X.-M. Chen, MD, Department of Medical Microbiology and Immunology, Creighton University School of Medicine, Criss III, Room 352, 2500 California Plaza, Omaha, NE 68178 (xianmingchen@creighton.edu).

The Journal of Infectious Diseases® 2018;218:1336–47

© The Author(s) 2018. Published by Oxford University Press for the Infectious Diseases Society of America. All rights reserved. For permissions, e-mail: journals.permissions@oup.com. DOI: 10.1093/infdis/jiy299

of the parasite Cdg7_FLc_1000 (GenBank ID: FX115830.1) [11] causes trans-suppression of host sphingomyelin phosphodiesterase 3 (*SMPD3*) gene, resulting in attenuation of cell migration of infected host cells [7]. The *dickkopf* (*Dkk*) family encodes secreted proteins and consists of 4 main members in vertebrates (ie, *Dkk1,2,3,4*) [12]. *Dkk1*, a secreted protein with 2 cysteine rich regions, is involved in embryonic development [12] and in the regulation of intestinal epithelial cell migration [13]. Induction of *Dkk1* was previously demonstrated in human intestinal epithelial cells following *C. parvum* infection [14]. Here, we report that host delivery of parasite Cdg7_FLc_1030 RNA (GenBank ID: FX115613.1) [11] promotes the transcription of *Dkk1* gene in infected intestinal epithelial cells; release of *Dkk1* from host cells during *C. parvum* infection is involved in inhibition of cell migration of epithelial cells, including noninfected bystander cells.

METHODS

C. parvum and Cell Lines

C. parvum oocysts of the Iowa strain were purchased from a commercial source (Bunch Grass Farm, Deary, ID). The human nonmalignant intestinal epithelial cell line (INT; FHs 74 Int, CCL-241) was purchased from ATCC (Manassas, VA). The murine intestinal epithelial cell line (IEC4.1) was a kind gift from Dr. Pingchang Yang (McMaster University, Hamilton, ON, Canada) and cultured as previously reported [7].

Infection Models and Infection Assays

Models of intestinal cryptosporidiosis using cell lines were employed as previously described; infection was with a 1:1 ratio of *C. parvum* oocysts and host cells [7, 11]. An ex vivo infection model employing enteroids from neonatal mice [15] and a well-developed infection model of cryptosporidiosis in neonatal mice [16, 17] were used for ex vivo and in vivo experiments. At least 5 animals from each group were sacrificed and ileal tissues were obtained for immunohistochemistry and biochemical analyses. Real-time polymerase chain reaction (PCR), immunofluorescence microscopy, and immunohistochemistry were used to assay *C. parvum* infection as previously reported [18, 19]. Details are described in the [Supplementary Materials](#).

Quantitative Real-Time PCR

For quantitative analysis of mRNA and *C. parvum* RNA expression, comparative real-time PCR was performed as previous reported [20] using the SYBR Green PCR Master Mix (Applied Biosystems, Carlsbad, CA). Briefly, RNA was extracted using TRI-reagent, treated with DNA-free Kit (Ambion) to remove any remaining DNA. Quantified 500 ng RNA was reverse-transcribed using T100 thermal cyclers (Bio-Rad). Real-time PCR was then performed using 25 ng of template cDNA for each RNA gene of interest. Each sample was run in triplicate. The relative abundance of each RNA was calculated using the $\Delta\Delta C_t$ method and normalized to *GAPDH* or U2 small nuclear RNA

(*RNU2-1*) (a nuclear RNA). The sequences for all the primers are listed in [Supplementary Table 1](#).

siRNAs and Plasmids

Custom-designed siRNA oligos against Cdg7_FLc_1030 and a scrambled siRNA were synthesized by Integrated DNA Technologies (Coralville, IA) and transfected into cells with Lipofectamine RNAimax (Invitrogen). Sequences of siRNAs are: 5'-CGUCAAGGAAUUUACGUAUUU-3' for Cdg7_FLc_1030 and nonspecific scrambled sequence 5'-UUCUCCGAACGUGUCACGUUU-3' for the control. The plasmids expressing parasite RNAs were generated by real-time PCR amplification of the cDNA, using RNA from *C. parvum* sporozoites and cloned into the pcDNA3.1(+) vector, per the manufacturer's protocol (Invitrogen). The sequences for all the primers are listed in [Supplementary Table 1](#).

Whole Cell Extracts, Western Blot, and Immunofluorescent Staining

Whole cell extracts were prepared using the Mammalian Protein Extraction Reagent (Fisher) supplemented with cocktail protease inhibitors. Cell pellets were incubated in the Mammalian Protein Extraction Reagent, centrifuged at 16 100g for 20 minutes and the supernatants were saved as the whole cell extracts, as previously reported [21]. Details for western blot and immunofluorescent staining are described in the [Supplementary Materials](#).

RNA Immunoprecipitation, Chromatin IP, and Chromatin Isolation by RNA Purification Analyses

The formaldehyde cross-linking RNA immunoprecipitation (RIP) was performed as described [22]. For chromatin immunoprecipitation (ChIP) analysis, a commercially available ChIP Assay Kit (Upstate Biotechnologies) was used in accordance with the manufacturer's instructions. Chromatin isolation by RNA purification (ChIRP) analysis was performed as previously reported [23]. A pool of tiling oligonucleotide probes with affinity specific to the *C. parvum* Cdg7_FLc_1030 RNA sequences was used and glutaraldehyde cross-linked for chromatin isolation. The sequences for all the primers and probes are listed in [Supplementary Table 1 and Table 2](#). Details are described in the [Supplementary Materials](#).

Cell Migration and MTT Assay

The wound-healing assay was used to analyze cell migration. Cell proliferation assay was carried out using the CellTiter 96 AQueous One Solution Cell Proliferation 3-(4,5-dimethylthiazol-2-yl)-2,5-diphenyltetrazolium bromide (MTT) Assay Kit (Promega Corporation), with details in the [Supplementary Materials](#).

RESULTS

C. parvum Infection Attenuates Intestinal Epithelial Cell Migration in Both Directly Infected Cells and Noninfected Bystander Cells

In our previous studies, we demonstrated that *C. parvum* infection of cultured human intestinal epithelial cells inhibited

cell migration and inhibition of migration was not limited to directly infected cells [7]. Inhibition of host cell migration during infection was observed in both directly infected cells and bystander noninfected cells using cultured murine intestinal epithelial cells (IEC4.1 cells) (Figure 1A–1C). To confirm that infection can attenuate cell migration of noninfected bystander cells, we collected the supernatants from IEC4.1 cell cultures after exposure to *C. parvum* infection for 24 and 48 hours and took a centrifugation approach to remove cell or parasite debris. IEC4.1 cells also showed attenuation of migration after culture with the conditioned media with the supernatants (Figure 1A and 1C). This decrease in cell migration distance was not due to cell death induced by infection [24, 25], as the MTT assay revealed no obvious difference in cell number between the infected cell cultures and the noninfected control (Figure 1D and Supplementary Figure 1). Lack of obvious cell death may reflect the higher infection rate and the fully confluent nature of the cell cultures, as *C. parvum*-infected cells and confluent cultures are resistant to apoptotic cell death [25].

C. parvum Infection Induces Expression and Release of Dkk1 from Infected Intestinal Epithelial Cells

Given the inhibitory effect of supernatant from infected cultures on epithelial cell migration, we questioned whether soluble factors in the supernatant released from infected cells are involved in the underlying mechanisms. Genome-wide mRNA array analysis in previous studies revealed significant alterations in gene expression profiles in nonmalignant (INT) and malignant (HCT-8) human intestinal epithelial cells after *C. parvum* infection in vitro [10, 14, 26]. Genes that are upregulated in host cells include cytokine/chemokine genes and *DKK1* gene. There are 4 members of the DKK protein family, that is DKK1–4, conserved in humans and mice [12]. Based on our previous genome-wide array analysis [10], upregulation of DKK1, but not DKK2–4, was shown in INT cells at 48 hours after *C. parvum* infection (Figure 2A). Similarly, upregulation of DKK1, but not DKK2–4, was observed in INT and IEC4.1 cells after exposure to *C. parvum* for various periods of time using real-time PCR (Figure 2B). Interestingly, a

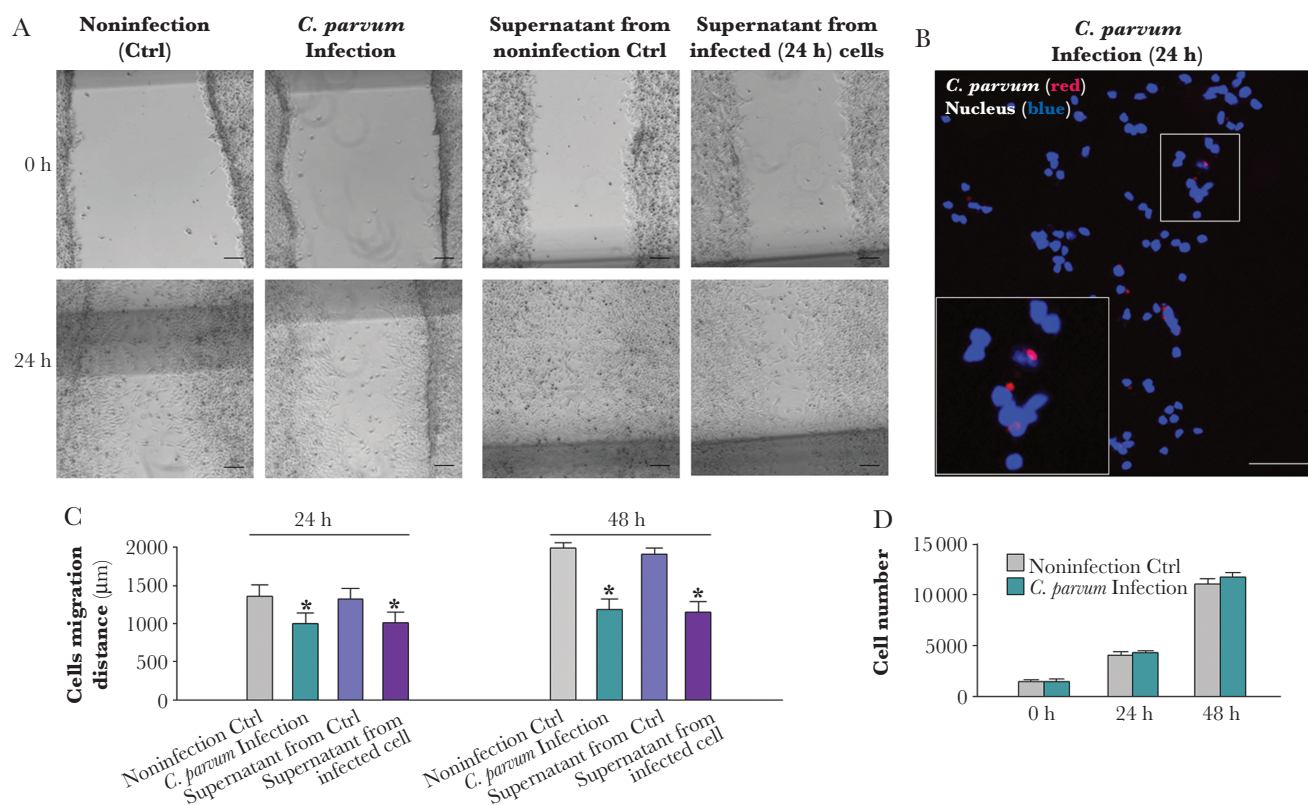


Figure 1. Inhibition of intestinal epithelial cell migration during *Cryptosporidium parvum* infection. *A*, Decreased migration of IEC4.1 cells following *C. parvum* infection or after incubation with the supernatants from infected IEC4.1 cultures. Cell migration was assessed by measurement of the distance of cell migration after the wound-healing assay. Representative phase images of cell cultures after exposure to *C. parvum* infection or incubation with the conditioned supernatants for 24 hours are shown. *B*, Representative dual fluorescent image of cell cultures after exposure to *C. parvum* infection for 24 hours, showing presence of infected cell (parasite stained in red) and noninfected cells at the migrating edge. Nuclei of cells were stained blue with DAPI (4',6-diamidino-2-phenylindole). *C*, Quantitative analysis of the migration distance of IEC4.1 cells following *C. parvum* infection or after incubation with the supernatants from infected IEC4.1 cultures. *D*, Quantitative analysis of the cell numbers in the IEC4.1 cultures following *C. parvum* infection. Data represent means \pm SEs from 3 independent experiments. * $P < .01$ ANOVA versus noninfected control (Ctrl).

slight decrease in expression levels of *Dkk2* (in INT cells at 48 hours postinfection) and *Dkk3* (in IEC4.1 cells at both 24 and 48 hours postinfection) was measured. Using an ex vivo infection model employing enteroids from neonatal mice [15], we detected an increased expression level of *Dkk1* RNA in enteroids following *C. parvum* infection (Figure 2C). An increase in *Dkk1* expression was also observed in the intestinal epithelium in infected neonatal mice following oral administration of the parasite (Figure 2C). Different from results with the ex vivo infection model, a higher *Dkk1* increase at 48 hours than at 24 hours postinfection was observed in the intestinal epithelium in infected neonatal mice, probably due to the different time course of infection in the 2 models [15]. Moreover, upregulation of *Dkk1* at the protein level, but not *Dkk2*–4, was further confirmed in IEC4.1 cell cultures directly exposed to

C. parvum or in supernatants from the cell cultures after exposure to *C. parvum* infection (Figure 2D).

Dkk1 Released From Infected Epithelial Cells in the Supernatants Is Involved in *C. parvum*-Induced Inhibition of Cell Migration of the Noninfected Bystander Cells

To explore whether DKK1 released from infected cells is involved in inhibition of epithelial cell migration during *C. parvum* infection, we used a neutralizing antibody to *Dkk1* [27] and measured its effects on cell migration associated with *C. parvum* infection. The neutralizing antibody to *Dkk1* restored cell migration of IEC4.1 cells after incubation with the supernatants of infected cell cultures (Figure 3A and 3B). In accordance, as a positive control, addition of recombinant mouse *Dkk1* protein to the culture media inhibited the migration of IEC4.1 cells (Figure 3C).

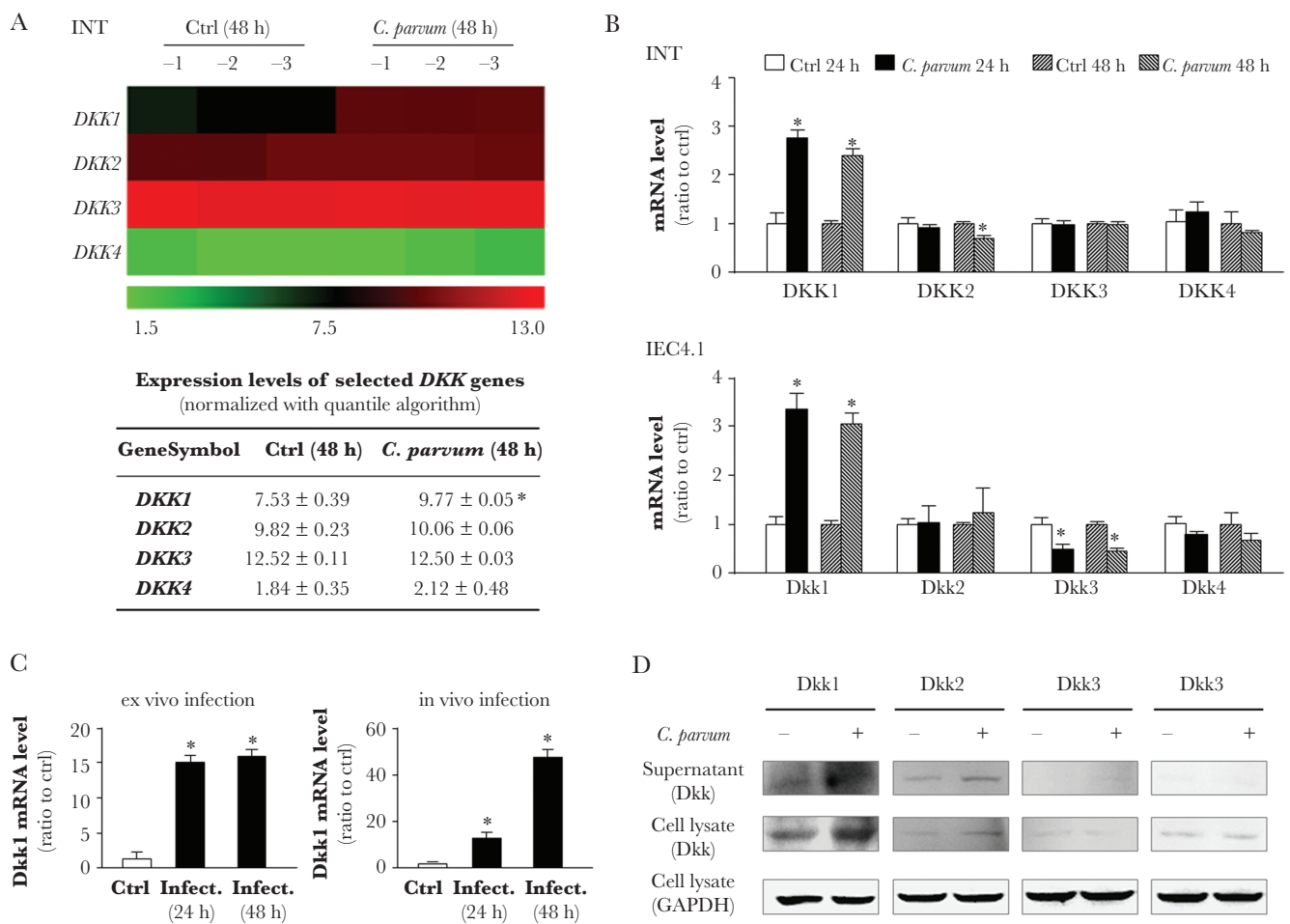


Figure 2. *Cryptosporidium parvum* infection induces expression and release of *Dkk1* from infected intestinal epithelial cells. **A**, Alterations in *DKK* gene expression profile from genome-wide transcriptome analysis in INT cells following *C. parvum* infection from our previous study (the GEO database GSE87047) [10]. INT cells were exposed to *C. parvum* infection for 48 hours, followed by the microarray analysis; noninfected cells were used as the control (Ctrl). The mean value of the expression level for *DKK* genes is presented as a heatmap and listed in the table. **B**, Alterations in *DKK* gene expression in INT cells and IEC4.1 following *C. parvum* infection. INT and IEC4.1 cells were exposed to *C. parvum* infection for 24–48 hours, followed by real-time PCR analysis; noninfected cells were used as the control. **C**, Induction of *Dkk1* gene in the enteroids following ex vivo *C. parvum* infection (Infect.) and in ileum tissues of neonates following in vivo *C. parvum* infection. Expression levels of *Dkk1* gene in enteroids at 24 and 48 hours after ex vivo infection, as well as in the ileum epithelium at 24 and 48 hours after in vivo infection, were measured using real-time PCR. **D**, Upregulation of *Dkk1* at the protein level, but not for *Dkk2*–4, in IEC4.1 cell cultures directly exposed to *C. parvum* or in supernatants from the cell cultures after exposure to *C. parvum* infection. The blotting gels were also stained for protein with silver staining as control. Data represent means ± SEs from 3 independent experiments. **P* < .01 ANOVA versus non-infected control.

Delivery of Parasite Cdg7_FLC_1030 RNA to Infected Epithelial Cells Triggers Transactivation of Host *Dkk1* Gene During *C. parvum* Infection

Our previous studies demonstrate that a panel of *C. parvum* RNA transcripts is selectively delivered into epithelial cells during host cell invasion and may modulate gene transcription in infected cells [10]. We generated constructs expressing each of these *C. parvum* RNAs and transfection of each of these constructs resulted in significant expression of the corresponding parasite RNA in IEC4.1 cells (Supplementary Figure 2). Expression levels of *Dkk1* were then measured, by real-time PCR, in IEC4.1 cells after transfection of these constructs. Interestingly, a high level of *Dkk1* RNA was detected in cells following transfection of parasite Cdg7_FLC_1030, an RNA transcript from the chromatin 7 of low protein-coding potential (GenBank ID: FX115613.1) [21, 22] (Figure 4A and 4B). No significant alteration in *Dkk1* expression was detected in cells transfected with the other parasite RNA transcripts (Supplementary Figure 3). We then questioned whether nuclear delivery of Cdg7_FLC_1030 causes *Dkk1* transcription. Because conventional genetic tools are very difficult, if not impossible, to modify *C. parvum* genes [1, 28], we developed a method to treat cells with an siRNA to Cdg7_FLC_1030 for 4 hours and then exposed them to *C. parvum*. The increase in Cdg7_FLC_1030 RNA level in cells induced by *C. parvum* infection was significantly suppressed by pretreatment with the siRNA to Cdg7_FLC_1030 (Figure 4C). Accordingly, upregulation of *Dkk1* RNA expression induced by *C. parvum* infection was at least partially inhibited through pretreatment of the siRNA to Cdg7_FLC_1030 (Figure 4C).

To explore how Cdg7_FLC_1030 may promote *Dkk1* expression in the host cells, we measured the enrichment of transcriptional activity markers within the promoter region of the *Dkk1* gene locus in cells following infection. Histone modifications, such as H3K4 and H3K36 methylations, are generally associated with gene transcriptional activation [20]. Increased enrichment of H3K4me1 and H3K36me3 was detected in the *Dkk1* gene locus in infected cells using ChIP analysis with anti-H3K4me1 or anti-H3K36me3 and the PCR primer sets designed to cover the various promoter regions of the *Dkk1* gene locus (Figure 5A). In addition, increased enrichment of the RNA polymerase II (Pol II) was also detected in the *Dkk1* gene locus in infected cells using ChIP analysis with anti-Pol II and the same PCR primer sets (Figure 5A). To test whether Cdg7_FLC_1030 is assembled into the Pol II complex in the infected cells, we performed RIP analysis of infected cells. A significant amount of Cdg7_FLC_1030, but not the control RNU-2 RNA, was detected in the immunoprecipitates from infected cells using anti-Pol II (Figure 5B). To define whether Cdg7_FLC_1030 is physically recruited to the *Dkk1* gene locus in infected cells, we used a pool of biotinylated tiling oligonucleotide probes specific to Cdg7_FLC_1030 for ChIRP analysis. Recruitment of Cdg7_FLC_1030 was detected within the promoter region of the *Dkk1* gene locus

in cells following infection (Figure 5C). To further explore how Cdg7_FLC_1030 may activate transcription of the *Dkk1* gene, we generated various luciferase reporter vectors encompassing the various upstream regions of the transcription start site of the *Dkk1* gene (Figure 5D). IEC4.1 cells were transfected with the luciferase reporter plasmids, followed by exposure to *C. parvum* infection. No significant increase in luciferase activity associated with the *Dkk1* promoter regions was detected in cells following infection (Figure 5D). In contrast, a marked increase in luciferase activity associated with the human interleukin 8 luciferase reporter plasmid, as a positive control for *C. parvum*-induced transcription of host genes [29], was measured in infected cells (Figure 5D). Because the luciferase reporter assay cannot mimic the chromatin-remodeling-mediated regulation of gene transcription, we speculate that Cdg7_FLC_1030 may activate transcription of the *Dkk1* gene through modulation of chromatin-remodeling-associated histone modifications.

DKK1-Mediated Suppression of Host Cell Migration during *C. parvum* Infection Involves Inhibition of Cdc42/Par6 Signaling

Previous studies demonstrated that *Dkk1* mediates cell migration through inhibition of Cdc42/Par6 signaling [13]. To define whether Cdc42/Par6 signaling is involved in *C. parvum*-induced inhibition of intestinal epithelial cell migration, we performed immunostaining of Cdc42-active and Par6 in IEC4.1 cell cultures upon wound healing after incubation with supernatants from infected cell cultures. An increased staining of Cdc42-active and Par6 was detected in cells along the migrating edge after wounding when they were cultured with normal control media (Figure 6A and 6B). In contrast, we detected a weakened staining of both Cdc42-active and Par6 in cells along the migrating edge upon wounding in the cell cultures after incubation with the conditioned supernatants (Figure 6A and 6B). Addition of neutralizing anti-*Dkk1* to the culture media restored the staining level of Cdc42-active and Par6 in cells along the migrating edge (Figure 6A and 6B). Decreased staining of Cdc42-active and Par6 along the migrating edge was also detected in cells following culture with addition of the recombinant mouse *Dkk1* (Supplementary Figure 4).

DISCUSSION

In this study, we report that host delivery of a parasite Cdg7_FLC_1030 RNA transcript into infected intestinal epithelial cells during *C. parvum* infection activates transcription of the *Dkk1* gene and increases release of *Dkk1* protein from host epithelial cells. Consequently, induction and release of *Dkk1* inhibits cell migration of both infected cells and noninfected bystander cells. Coupled with our previous study on the trans-suppression of the *Smpd3* gene through Cdg7_FLC_1000-mediated epigenetic suppression to inhibit cell migration in infected cells [7], our data support the hypothesis that delivery of parasite RNA transcripts into infected host cells during *Cryptosporidium*

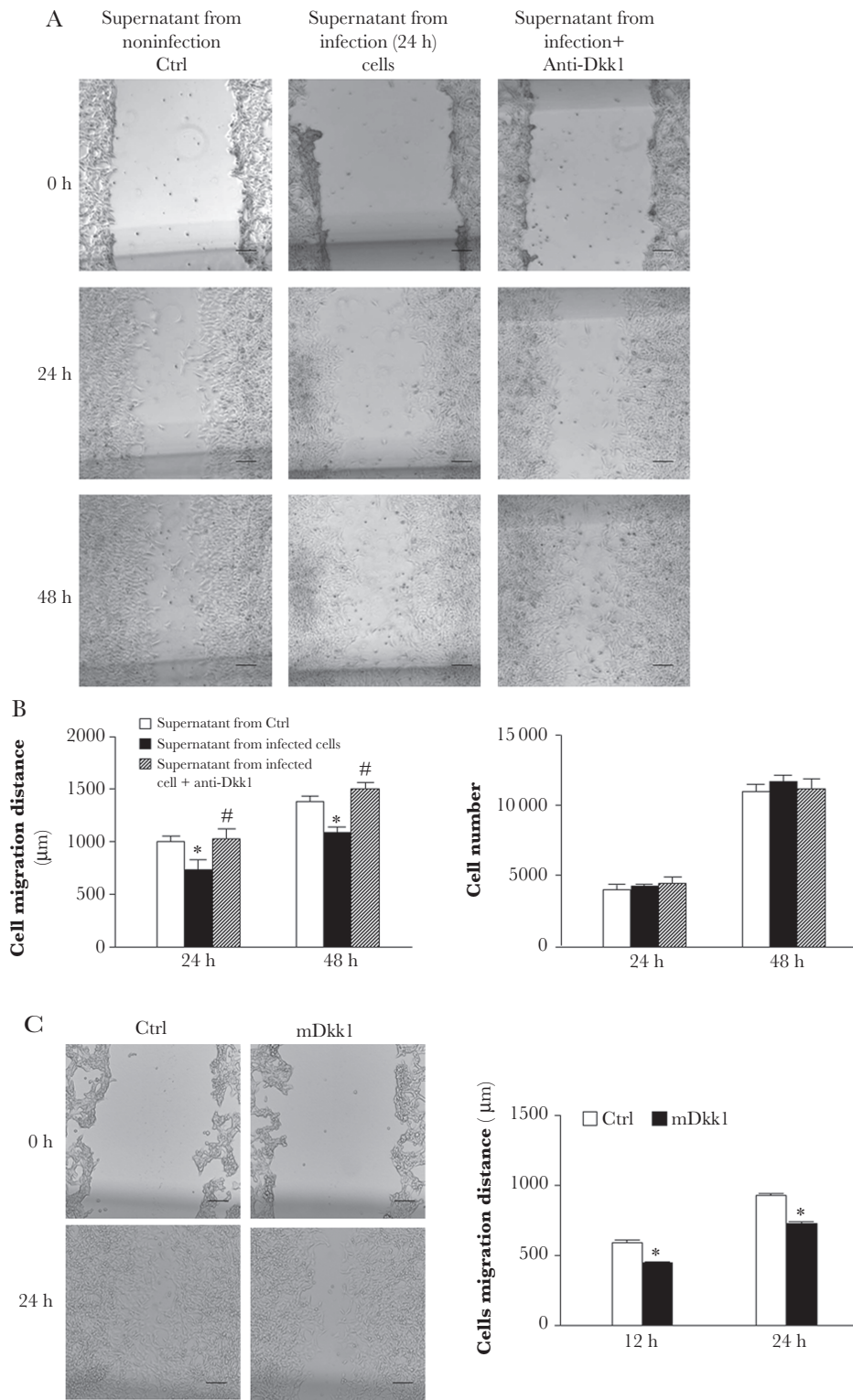


Figure 3. Release of Dkk1 in the supernatants is involved in *Cryptosporidium parvum*-induced inhibition of cell migration of the noninfected bystander cells. *A*, Representative phase images of IEC4.1 cell cultures after incubation with the supernatants from infected IEC4.1 cultures for 24–48 hours, in the presence or absence of neutralizing anti-Dkk1. Cell migration was assessed by measurement of the distance of cell migration after the wound-healing assay. *B*, Quantitative analysis of the migration distance of IEC4.1 cells after incubation with the supernatants from infected IEC4.1 cultures, in the presence or absence of neutralizing anti-Dkk1. Proliferation of IEC4.1 cells after incubation with supernatants from infected IEC4.1 cultures, in the presence or absence of the neutralizing anti-Dkk1, was also assessed by 3-(4,5-dimethylthiazol-2-yl)-2,5-diphenyltetrazolium bromide (MTT) assay. *C*, Inhibition of IEC4.1 migration by recombinant mDkk1. The migration distance of IEC4.1 cells, in the presence or absence of the recombinant mouse Dkk1 (mDkk1), was measured and cell proliferation assessed by MTT assay. Data represent means \pm SEs from 3 independent experiments. * $P < .01$ ANOVA versus cells treated with supernatant from noninfected control (Ctrl) or the non-antibody treated Ctrl; # $P < .01$ ANOVA versus cells after incubation with the supernatants in the absence of anti-Dkk1 treatment.

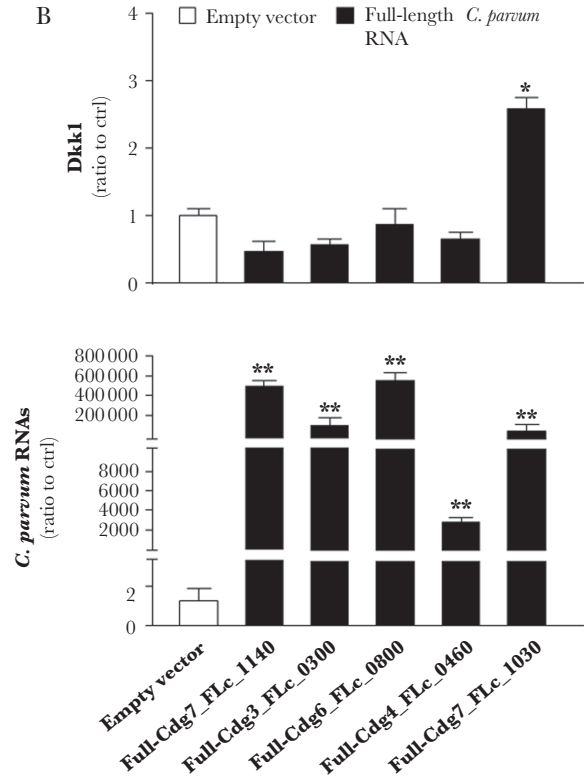
A *Cdg7_Flc_1030*



```

AGAAAAAAAAACATTCCTTTTAAAAAATAAATCCTTTAATTATAAGATAAT
AATTTTGTGTAAGTGAATAAGTTACATATAGATGAATTGAATATCTT
TGAATTTGATTATATTGCTTTTATAGATTATTAGAATCTCGCAAGGT
TCCTCTACTTTGAAAAATTAATTAATTAACAATAATTCAAACCTTTTCA
TCCAGGGATCAATAACAATTATAATTAACAAGGATTATACAGA
ATATTGAGCAAATATGATAGGGAGAAAGATATTGAAAAATCTTTGCCT
TTATAAATCTGTAATATTAGTCAAATGCTTCTCTAAACTATATGGC
TCATTATCAAAGTGTAGCTGTGAATATTAACCTAAACTCTATGCCCT
TACTGCAATACTCATACCTCCCTTTTCCAATAGTTAGTAATCTATAGGA
ATAATATTTACAAAAGAAGAAAGCAAACATTAGGAAGAAAGAAAT
TATTTATAGCATATTTCTATTAATATTTATTCATTAGTTTGGATACT
TTTCATGTTAATAATAGAAATTTGTAATAATCAACCTCACATCACCAT
ATTGTGCAATGTTTCTCCTTCTAAATACTTAATTTACTCATCTTAA
CAACGGTACCTTTTCACTAACATAAATACCGTCAAGGAATTTACGTA
TATCTTTAATTTCTGCAAGAGCGCATTGGTGAATCAAAGCAGCAGAA
CGAGATACAAGCTCTAAATCAGTACCTGTAATGATTAACCTCGTCCTTA
ACAGAGTTAGATTTCTCAACAACAACCTCTGGAAGCATCTTAACAGT
TCTGACCTCTTCTCTCCAAGAAGTTTCTGATTCAATCAAATGTC
CATTGTTTAAAGATATTTGAGTTAATTTGGAAGTGGGAATATACAAGC
GCATCTTATACTCAAATCTTCTATGACCAACCATCATGTTCTTGA
TTGCTGAACAGACAGTATTAATAGCTGATTGATGGCGTGGAGTACCG
AACCATACTTCAATTTCAACAACCTTACCATTACCACATAACTTAATAT
CTACCGGTAATGTTGAAAGATCTTGTAACCTGACCAAACTTTCCA
GTAACAGTAACGGTCTTAGACTTAACAGAAACTGTTGTTCTTCCATT
ACACGGAAATGATTCATAAGTGAAAATGTCCTTCAATTTTCTTCAA
TATTTAATTAATAAACTCGATGGATGTTATGTGTATATATATAAATTTAA
ATATTATTCGTAATCTTCCCTTATTAATAAACTGGCTCAAATTAAC
TCAGATTTATAAATCTTTGTCATCTT
    
```

B



C

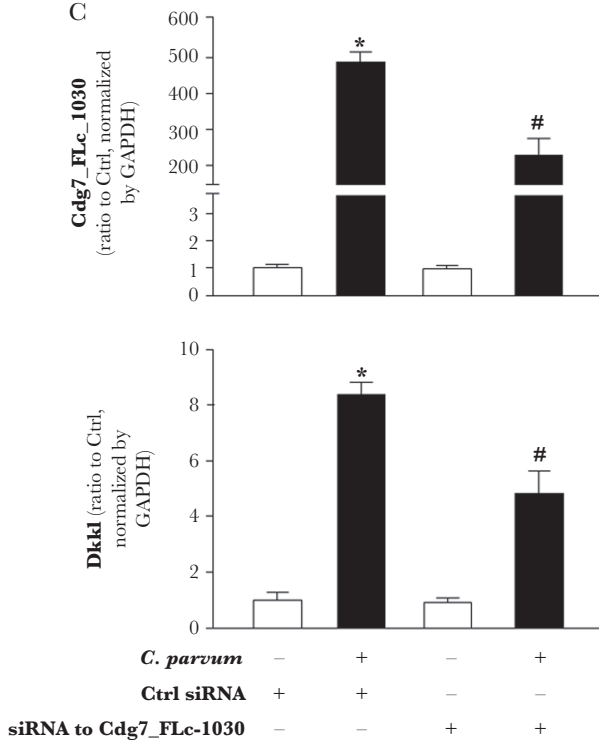


Figure 4. Induction of the *Dkk1* gene in epithelial cells following *Cryptosporidium parvum* infection is associated with delivery of *Cdg7_Flc_1030* into the host cells. A, Chromatic location and sequence of the *Cdg7_Flc_1030* gene in *C. parvum*. B, Expression of Full-*Cdg7_Flc_1030*, but not other parasite RNAs, resulted in induction of *Dkk1* expression in IEC4.1 cells. IEC4.1 was transfected with the constructs expressing various full-lengths of parasite RNAs for 48 hours. Cells transfected with the empty vector were used as the control. Whole-cell extracts were collected and expression levels of corresponding parasite RNAs and *Dkk1* were measured with real-time PCR. C, Inhibition of *Cdg7_Flc_1030* in host cells by the siRNA treatment attenuated the induction of *Dkk1* following *C. parvum* infection. IEC4.1 cells were treated with a siRNA to *Cdg7_Flc_1030* for 12 hours and then exposed to *C. parvum* infection for additional 24 hours. A nonspecific scrambled siRNA was used as the control (Ctrl). Contents of *Cdg7_Flc_1030* and *Dkk1* cells were quantified by real-time PCR. Data represent means \pm SEs from 3 independent experiments. * $P < .01$ ANOVA versus noninfected cells treated with the control siRNA or empty vector controls; # $P < .01$ ANOVA versus infected cells treated with the control siRNA.

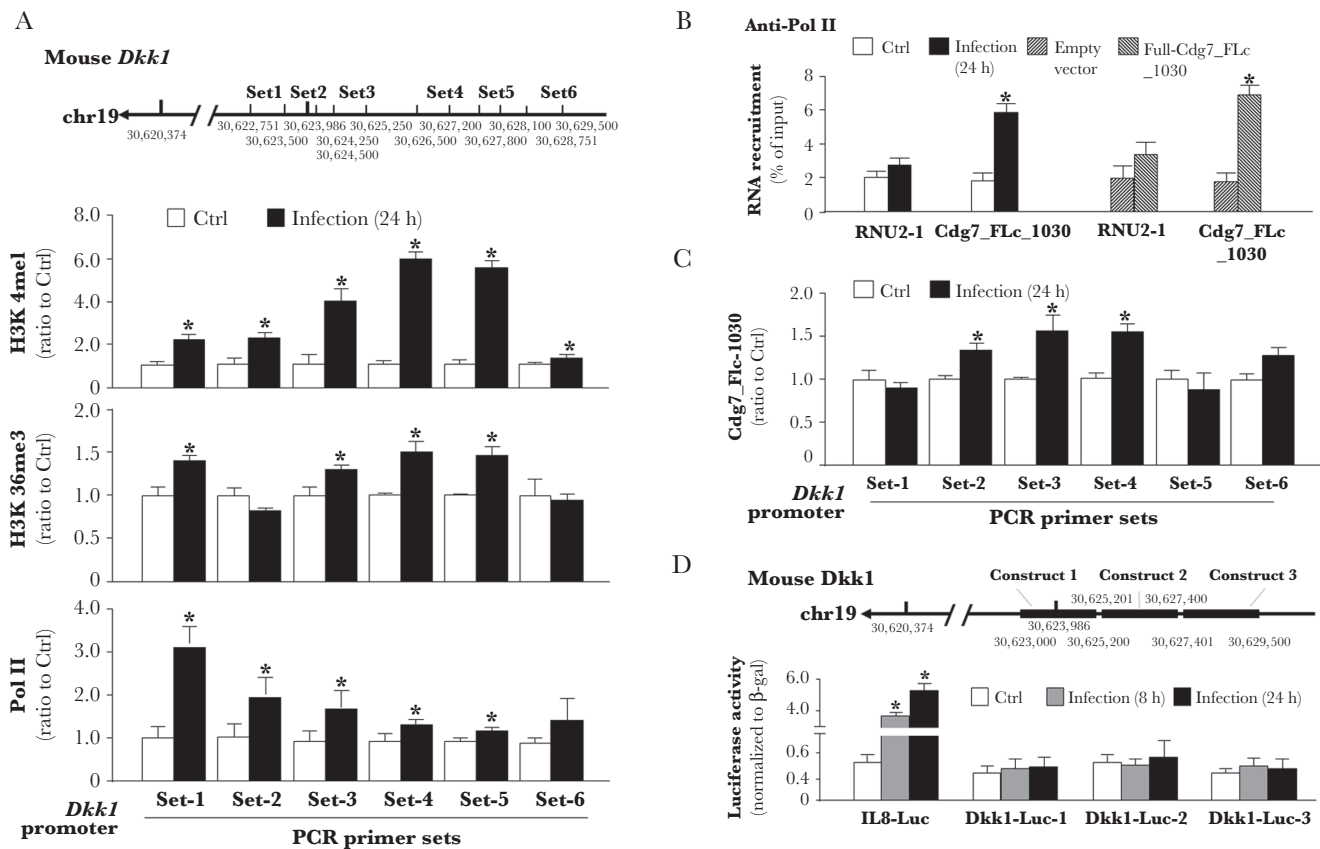


Figure 5. Host delivery of Cdg7_FLc_1030 triggers transcription of the *Dkk1* gene in epithelial cells. **A**, Levels of the transcription activity markers, H3K4me1 and H3K36me3, as well as enrichment of Pol II, associated with the *Dkk1* gene locus in IEC4.1 cells following *Cryptosporidium parvum* infection. Cells were exposed to *C. parvum* infection for 24 hours, followed by chromatin immunoprecipitation (ChIP) analysis using anti-H3K4me1, anti-H3K36me3, or anti-Pol II, respectively, and the PCR primer sets as designed. Increased enrichment of H3K4me1 and H3K36me3, as well as Pol II, was detected in the *Dkk1* gene locus in cells following infection. **B**, Assembly of Cdg7_FLc_1030 to the Pol II complex in cells following *C. parvum* infection. IEC4.1 were exposed to *C. parvum* infection for 24 hours or transfected with Full-Cdg7_FLc_1030 for 24 hours, followed by RNA immunoprecipitation (RIP) analysis using anti-Pol II and PCR primers for Cdg7_FLc_1030. Assembly of the U2 RNA was also measured as control (Ctrl). **C**, Recruitment of Cdg7_FLc_1030 to the *Dkk1* gene locus in IEC4.1 cells following *C. parvum* infection. Cells were exposed to *C. parvum* infection for 24 hours, following by chromatin isolation by RNA purification (ChIRP) analysis using a pool of probes specific to Cdg7_FLc_1030 and the PCR primer sets as designed. Increased recruitment of Cdg7_FLc_1030 was detected in the *Dkk1* gene locus in cells following infection. **D**, *C. parvum* infection did not promote the luciferase activity associated with the transcription of the *Dkk1*-promoter luciferase reporter constructs. Various regions of *Dkk1* promoter were cloned into the luciferase reporter constructs and the interleukin 8 luciferase reporter (IL8-Luc) plasmid containing human IL8 promoter was used for the positive control. IEC4.1 cells were transfected with the constructs for 12 hours and followed by exposure to *C. parvum* infection for 24 hours. Cells transfected with the empty vector were used as the control. The luciferase activities of the cells were then measured and normalized to β-gal. Data represent means ± SEs from 3 independent experiments. * $P < .01$ ANOVA versus noninfected or empty vector controls.

infection causes inhibition of epithelial cell migration of both infected and noninfected bystander cell populations, contributing to disturbances of intestinal epithelial homeostasis following *Cryptosporidium* infection (Figure 7).

Consistent with data from previous studies [10, 14], we detected induction of *Dkk1*, but not other members of the *Dkk* family, in intestinal epithelial cells after *C. parvum* infection, using in vitro, ex vivo, and in vivo infection models. Interestingly, tissue damage itself can cause an upregulation of *Dkk-1* and production of *Dkk-1* is a normal response to manage tissue remodeling in response to injury [30–32]. Increased amounts of *Dkk1* have also been reported in chronic inflammatory diseases such as various types of cancers, rheumatoid arthritis, and lupus [33–35]. Here, our data indicate that

C. parvum infection of intestinal epithelial cells triggers *Dkk1* transcription via host delivery of Cdg7_FLc_1030, a parasite RNA transcript of low protein potential [11]. This induction of *Dkk1* through host delivery of Cdg7_FLc_1030 appears to be specific as expression of other parasite RNA transcripts, even though they were also delivered into infected host cells, failed to induce *Dkk1* transcription. Moreover, *Dkk1* induction was not detected in intestinal epithelial cells following infection by *Escherichia coli* or *Aeromonas caviae* [36, 37], suggesting that this is not a general intestinal epithelial cell response to pathogen infection or inflammatory stimulation.

Mechanistically, transactivation of the *Dkk1* gene in intestinal epithelial cells after *C. parvum* infection is associated with an increased methylation of H3K4 and H3K36 in its gene

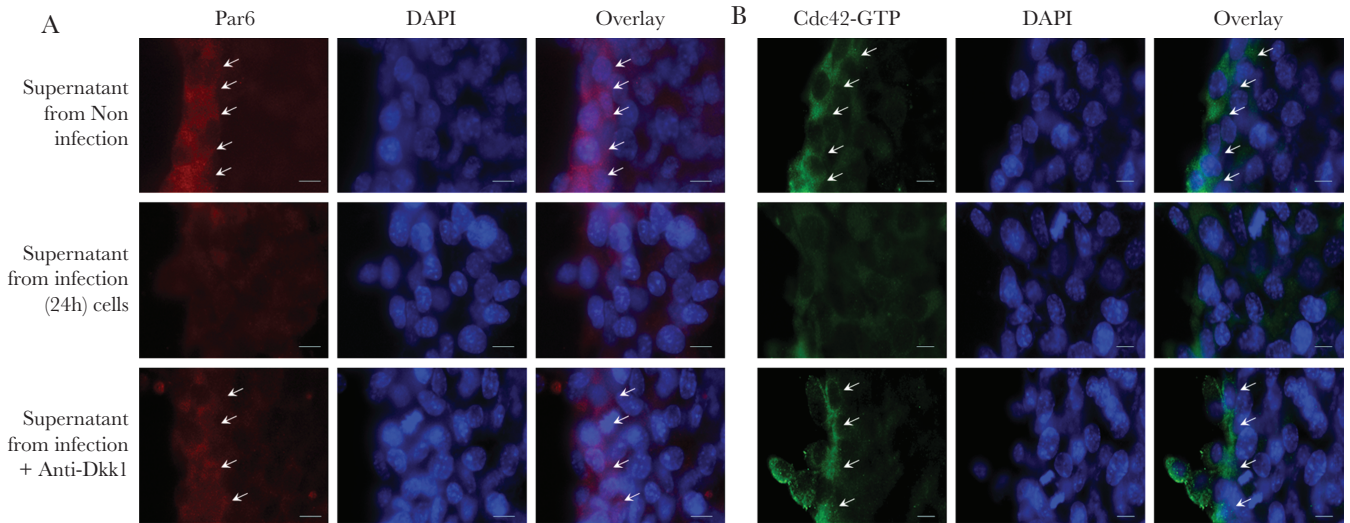


Figure 6. The Cdc42-Par6 signaling pathway is involved in DKK1-mediated suppression of host cell migration during *Cryptosporidium parvum* infection. IEC4.1 cells were incubated with the supernatants from infected IEC4.1 cultures for 24 hours, in the presence or absence of the neutralizing anti-Dkk1. Wound healing was applied to the cell cultured as the cell migration assay, followed by immunostaining with anti-Par6 or anti-Cdc42-GTP (Cdc42-active), respectively. Representative images showing the staining of Par6 (A) and Cdc42-GTP (B) in cells along the migrating edge (indicated by arrowheads) after wounding are shown. Data represent means \pm SEs from 3 independent experiments. Bar = 20 μ m.

promoter. We speculate that Cdg7_FLc_1030 may activate transcription of the *Dkk1* gene through modulation of chromatin-remodeling-associated histone modifications. Consistent

with the mechanism of transactivation for most genes in mammalian cells, the enrichment of Pol II to the *Dkk1* gene locus was also detected in cells following infection. It is still unclear

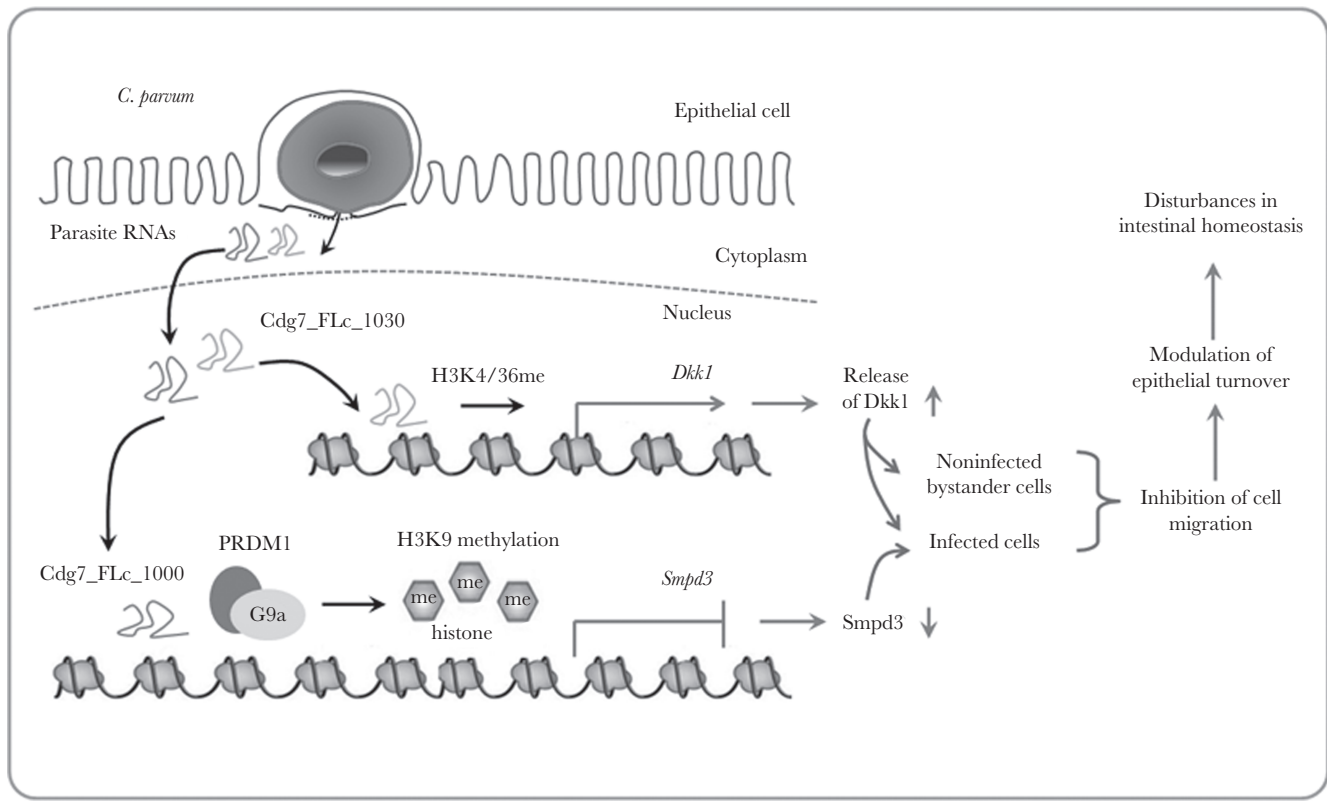


Figure 7. Delivery of parasite RNA transcripts into the nuclei of infected host epithelial cells following cryptosporidial infection activates transcription of the *Dkk1* gene (via delivery of Cdg7_FLc_1030) and suppresses the transcription of *Smpd3* gene (via delivery of Cdg7_FLc_1000) [7], resulting in the inhibition of epithelial cell migration of both infected host cells and noninfected bystander cells, a process that may benefit the parasite intracellular cell cycle in host cells.

how Cdg7_FLc_1030 RNA may trigger transcription of the *Dkk1* gene. Increasing evidence supports the hypothesis that RNA molecules in mammalian cells can function as scaffold molecules to affect gene transcription through their interactions with various RNA-binding components in the chromatin-remodeling complexes [38, 39]. As such, Cdg7_FLc_1030 may modulate the recruitment of those chromatin-remodeling complexes to the *Dkk1* gene locus. In our previous studies, we demonstrated that nuclear delivery of the parasite Cdg7_FLc_1000 transcript (GeneBank ID: FX115830.1) [11] causes trans-suppression of host *SMPD3* gene [7]. Cdg7_FLc_1000 can interact with the positive regulatory domain zinc finger protein 1, an RNA-binding protein with a role in the regulation of histone methylation [40, 41], and, consequently, causes trans-suppression of the *SMPD3* gene [7]. Another potential mechanism is that Cdg7_FLc_1030 may trigger *Dkk1* transcription through direct binding to a specific DNA motif in its promoter regions, as RNAs may interact directly with DNA molecules to form a triple-helical structure [38]. However, *C. parvum* infection failed to trigger luciferase activity in intestinal epithelial cells that were transfected with plasmids expressing the promoter region-(1/2/3) of the *Dkk1* gene locus.

Dkk1 was originally identified in the regulation of head formation of *Xenopus laevis* and is known to inhibit the canonical Wnt signaling pathway [42, 43]. Dkk1 is an antagonistic inhibitor of the Wnt signaling pathway that acts by isolating the Lrp5/6 receptors so that it cannot aid in activating the Wnt signaling pathway [44]. This inhibition plays a key role in heart, head, and forelimb development during anterior morphogenesis of the embryo [45]. A polarized localization of active Cdc42 and Par6 was demonstrated in the leading edge of migrating cells in cultured intestinal epithelial cells [13]. Dkk1 was reported to disrupt the polarized localization of active Cdc42 and Par6 in the leading edge of migrating cells, resulting in disturbance of cell migration [13]. In our experimental setting, increased staining of active Cdc42 and Par6 was observed in the migrating cells along the wounded edge. Our data also implicate the involvement of Cdc42/Par6 signaling in the attenuation of intestinal epithelial cell migration associated with release of Dkk1 during *C. parvum* infection. Dkk1 is a well-characterized Wnt signaling inhibitor and acts as an antagonist of the canonical Wnt pathway by binding to the Wnt receptor [46, 47]. Given the critical role of Wnt signaling in regulating intestinal epithelial cell migration [48, 49], future studies should investigate the potential role of Wnt signaling associated with Dkk1 release in inhibition of cell migration following infection. Cdg7_FLc_1030-mediated cell migration through induction and release of Dkk1 may be critical to the parasite intracellular cell cycle during intestinal infection, which merits *in vivo* investigation using cell-type specific Dkk1 knockout mice. Moreover, targeting Dkk1 may

be of relevance to the development of therapeutic strategies for intestinal cryptosporidiosis.

Supplementary Data

Supplementary materials are available at *The Journal of Infectious Diseases* online. Consisting of data provided by the authors to benefit the reader, the posted materials are not copyedited and are the sole responsibility of the authors, so questions or comments should be addressed to the corresponding author.

Notes

Acknowledgments. We thank Drs Quanghai Zhao (Northwest A&F University, China) and Shibin Ma (Creighton University) for helpful and stimulating discussions, and Barbara L. Bittner (Creighton University) for her assistance in writing the manuscript.

Financial Support. This work was supported by the National Institutes of Health (grant numbers A1116323 and A1136877 to X.-M. C.); Nebraska Department of Health and Human Services (grant number LB595 Cancer and Smoking Disease Research Program Development Grant to X.-M. C.); National Center for Research Resources (grant number G20RR024001); China Scholarship Council (to Z. M.); and National Natural Science Foundation of China (grant number 31372194 to Z. M.).

Potential conflicts of interest. All authors: No reported conflicts of interest. All authors have submitted the ICMJE Form for Disclosure of Potential Conflicts of Interest. Conflicts that the editors consider relevant to the content of the manuscript have been disclosed.

References

1. Striepen B. Parasitic infections: time to tackle cryptosporidiosis. *Nature* **2013**; 503:189–91.
2. O'Donoghue PJ. *Cryptosporidium* and cryptosporidiosis in man and animals. *Int J Parasitol* **1995**; 25:139–95.
3. Checkley W, White AC Jr, Jaganath D, et al. A review of the global burden, novel diagnostics, therapeutics, and vaccine targets for *Cryptosporidium*. *Lancet Infect Dis* **2015**; 15:85–94.
4. Barker N. Adult intestinal stem cells: critical drivers of epithelial homeostasis and regeneration. *Nat Rev Mol Cell Biol* **2014**; 15:19–33.
5. Creamer B, Shorter RG, Bamforth J. The turnover and shedding of epithelial cells. I. The turnover in the gastro-intestinal tract. *Gut* **1961**; 2:110–8.
6. Chen XM, Keithly JS, Paya CV, LaRusso NF. Cryptosporidiosis. *N Engl J Med* **2002**; 346:1723–31.
7. Ming, ZP, Gong AY, Wang Y, et al. Involvement of *Cryptosporidium parvum* Cdg7_FLc_1000 RNA in the attenuation of intestinal epithelial cell migration via trans-suppression of host cell *SMPD3* gene. *J Infect Dis* **2018**; 217:122–33.

8. Sateriale A, Striepen B. Beg, borrow and steal: three aspects of horizontal gene transfer in the protozoan parasite, *Cryptosporidium parvum*. *PLoS Pathog* **2016**; 12:e1005429.
9. Sibley LD. Intracellular parasite invasion strategies. *Science* **2004**; 304:248–53.
10. Wang Y, Gong AY, Ma S, et al. Delivery of parasite RNA transcripts into infected epithelial cells during *Cryptosporidium* infection and its potential impact on host gene transcription. *J Infect Dis* **2017**; 215:636–43.
11. Yamagishi J, Wakaguri H, Sugano S, et al. Construction and analysis of full-length cDNA library of *Cryptosporidium parvum*. *Parasitol Int* **2011**; 60:199–202.
12. Mukhopadhyay M, Shtrom S, Rodriguez-Esteban C, et al. Dickkopf1 is required for embryonic head induction and limb morphogenesis in the mouse. *Dev Cell* **2001**; 1:423–34.
13. Koch S, Capaldo CT, Samarín S, et al. Dkk-1 inhibits intestinal epithelial cell migration by attenuating directional polarization of leading edge cells. *Mol Biol Cell* **2009**; 20:4816–25.
14. Deng M, Lancto CA, Abrahamsen MS. *Cryptosporidium parvum* regulation of human epithelial cell gene expression. *Int J Parasitol* **2004**; 34:73–82.
15. Zhang XT, Gong AY, Wang Y, et al. *Cryptosporidium parvum* infection attenuates the *ex vivo* propagation of murine intestinal enteroids. *Physiol Rep* **2016**; 4:e13060.
16. Kapel N, Benhamou Y, Buraud M, Magne D, Opolon P, Gobert JG. Kinetics of mucosal ileal gamma-interferon response during cryptosporidiosis in immunocompetent neonatal mice. *Parasitol Res* **1996**; 82:664–7.
17. Lacroix S, Mancassola R, Naciri M, Laurent F. *Cryptosporidium parvum*-specific mucosal immune response in C57BL/6 neonatal and gamma interferon-deficient mice: role of tumor necrosis factor alpha in protection. *Infect Immun* **2001**; 69:1635–42.
18. Sasahara T, Maruyama H, Aoki M, et al. Apoptosis of intestinal crypt epithelium after *Cryptosporidium parvum* infection. *J Infect Chemother* **2003**; 9:278–81.
19. Zhou R, Gong AY, Eischeid AN, Chen XM. miR-27b targets KSRP to coordinate TLR4-mediated epithelial defense against *Cryptosporidium parvum* infection. *PLoS Pathog* **2012**; 8:e1002702.
20. Dong X, Weng Z. The correlation between histone modifications and gene expression. *Epigenomics* **2013**; 5:113–6.
21. Abmayr SM, Yao T, Parmely T, Workman JL. Preparation of nuclear and cytoplasmic extracts from mammalian cells. *Curr Protoc Mol Biol* **2006**; 35:12.3.1–12.3.10
22. Niranjankumari S, Lasda E, Brazas R, Garcia-Blanco MA. Reversible cross-linking combined with immunoprecipitation to study RNA-protein interactions in vivo. *Methods* **2002**; 26:182–90.
23. Chu C, Qu K, Zhong FL, Artandi SE, Chang HY. Genomic maps of long noncoding RNA occupancy reveal principles of RNA-chromatin interactions. *Mol Cell* **2011**; 44:667–78.
24. Liu J, Deng M, Lancto CA, Abrahamsen MS, Rutherford MS, Enomoto S. Biphasic modulation of apoptotic pathways in *Cryptosporidium parvum*-infected human intestinal epithelial cells. *Infect Immun* **2009**; 77:837–49.
25. Chen XM, Levine SA, Splinter PL, et al. *Cryptosporidium parvum* activates nuclear factor kappaB in biliary epithelia preventing epithelial cell apoptosis. *Gastroenterology* **2001**; 120:1774–83.
26. Yang YL, Serrano MG, Sheoran AS, Manque PA, Buck GA, Widmer G. Over-expression and localization of a host protein on the membrane of *Cryptosporidium parvum* infected epithelial cells. *Mol Biochem Parasitol* **2009**; 168:95–101.
27. Pozzi S, Fulciniti M, Yan H, et al. In vivo and in vitro effects of a novel anti-Dkk1 neutralizing antibody in multiple myeloma. *Bone* **2013**; 53:487–96.
28. Vinayak S, Pawlowic MC, Sateriale A, et al. Genetic modification of the diarrhoeal pathogen *Cryptosporidium parvum*. *Nature* **2015**; 523:477–80.
29. Zhou R, Hu G, Liu J, Gong AY, Drescher KM, Chen XM. NF-kappaB p65-dependent transactivation of miRNA genes following *Cryptosporidium parvum* infection stimulates epithelial cell immune responses. *PLoS Pathog* **2009**; 5:e1000681.
30. Price RM, Tulsyan N, Dermody JJ, Schwalb M, Soteropoulos P, Castronuovo JJ Jr. Gene expression after crush injury of human saphenous vein: using microarrays to define the transcriptional profile. *J Am Coll Surg* **2004**; 199:411–8.
31. Li X, Grisanti M, Fan W, et al. Dickkopf-1 regulates bone formation in young growing rodents and upon traumatic injury. *J Bone Miner Res* **2011**; 26:2610–21.
32. Koch S, Nava P, Addis C, et al. The Wnt antagonist Dkk1 regulates intestinal epithelial homeostasis and wound repair. *Gastroenterology* **2011**; 141:259–68, 268.e1–8.
33. Diarra D, Stolina M, Polzer K, et al. Dickkopf-1 is a master regulator of joint remodeling. *Nat Med* **2007**; 13:156–63.
34. Sato N, Yamabuki T, Takano A, et al. Wnt inhibitor Dickkopf-1 as a target for passive cancer immunotherapy. *Cancer Res* **2010**; 70:5326–36.
35. Wang XD, Huang XF, Yan QR, Bao CD. Aberrant activation of the WNT/ β -catenin signaling pathway in lupus nephritis. *PLoS One* **2014**; 9:e84852.
36. Ukena SN, Westendorf AM, Hansen W, et al. The host response to the probiotic *Escherichia coli* strain Nissle 1917: specific up-regulation of the proinflammatory chemokine MCP-1. *BMC Med Genet* **2005**; 6:43.
37. Hayes SL, Lye DJ, McKinstry CA, Vesper SJ. *Aeromonas caviae* strain induces Th1 cytokine response in mouse intestinal tract. *Can J Microbiol* **2010**; 56:27–31.
38. Ulitsky I, Bartel DP. lincRNAs: genomics, evolution, and mechanisms. *Cell* **2013**; 154:26–46.
39. Guttman M, Donaghey J, Carey BW, et al. lincRNAs act in the circuitry controlling pluripotency and differentiation. *Nature* **2011**; 477:295–300.

40. Gyory I, Wu J, Fejér G, Seto E, Wright KL. PRDI-BF1 recruits the histone H3 methyltransferase G9a in transcriptional silencing. *Nat Immunol* **2004**; 5:299–308.
41. Shin HM, Kapoor V, Guan T, Kaech SM, Welsh RM, Berg LJ. Epigenetic modifications induced by blimp-1 regulate CD8⁺ T cell memory progression during acute virus infection. *Immunity* **2013**; 39:661–75.
42. Cruciat CM, Niehrs C. Secreted and transmembrane wnt inhibitors and activators. *Cold Spring Harb Perspect Biol* **2013**; 5:a015081.
43. Glinka A, Wu W, Delius H, Monaghan AP, Blumenstock C, Niehrs C. Dickkopf-1 is a member of a new family of secreted proteins and functions in head induction. *Nature* **1998**; 391:357–62.
44. Lewis SL, Khoo PL, De Young RA, et al. Dkk1 and Wnt3 interact to control head morphogenesis in the mouse. *Development* **2008**; 135:1791–801.
45. Schneider VA, Mercola M. Wnt antagonism initiates cardiogenesis in *Xenopus laevis*. *Genes Dev* **2001**; 15:304–15.
46. Glinka A, Wu W, Delius H, Monaghan AP, Blumenstock C, Niehrs C. Dickkopf-1 is a member of a new family of secreted proteins and functions in head induction. *Nature* **1998**; 391:357–62.
47. Krupnik VE, Sharp JD, Jiang C, et al. Functional and structural diversity of the human Dickkopf gene family. *Gene* **1999**; 238:301–13.
48. de Lau W, Barker N, Clevers H. WNT signaling in the normal intestine and colorectal cancer. *Front Biosci* **2007**; 12:471–91.
49. Ouko L, Ziegler TR, Gu LH, Eisenberg LM, Yang VW. Wnt11 signaling promotes proliferation, transformation, and migration of IEC6 intestinal epithelial cells. *J Biol Chem* **2004**; 279:26707–15.